https://doi.org/10.5194/amt-2024-36
Preprint. Discussion started: 8 March 2024

Atmospheric Measurement Techniques Discussions

Optimal estimation of cloud properties from thermal infrared observations with a combination of deep learning and radiative transfer simulation

He Huang[1], Quan Wang[1], Chao Liu[2], Chen Zhou[1]

[1] School of Atmospheric Sciences, Nanjing University, Nanjing, 210023, China
[2] Collaborative Innovation Center on Forecast and Evaluation of Meteorological Disasters, Nanjing University of Information Science and Technology, Nanjing, 210044, China

Correspondence to: Chen Zhou (czhou17@nju.edu.cn)

Abstract. While traditional thermal infrared retrieval algorithms based on radiative transfer models (RTM) could not effectively retrieve the cloud optical thickness of thick clouds, machine learning based algorithms were found to be able to provide reasonable estimations for both daytime and nighttime. Nevertheless, stand-alone machine learning algorithms are occasionally criticized for the lack of explicit physical processes. In this study, RTM simulations and a machine learning algorithm are synergistically utilized using the optimal estimation (OE) method to retrieve cloud properties from thermal infrared radiometry measured by Moderate Resolution Imaging Spectroradiometer (MODIS). In the new algorithm, retrievals from a machine learning algorithm are used to provide the priori state for OE method, and an RTM is used to create radiance lookup tables that are used in the iteration processes. Compared with stand-alone OE, the cloud properties retrieved by the new algorithm show an overall better performance by optimizing the initial values. Compared with stand-alone machine-learning based algorithm, the radiances simulated based on retrievals from the new method align more closely with observations, and physical radiative processes are handled explicitly in the new algorithm. Therefore, the new method combines the advantages of RTM-based cloud retrieval methods and machine-learning models. These findings highlight the potential for machine-learning-based algorithms to enhance the efficacy of conventional remote sensing techniques.

1 Introduction

Clouds play an important role in the Earth's energy budget by altering radiation patterns at both the surface and the top of the atmosphere (TOA) (Liou and Davies, 1993; Stubenrauch et al.,2006). Cloud properties change in response to variations in greenhouse gases, aerosol concentrations, and global

https://doi.org/10.5194/amt-2024-36
Preprint. Discussion started: 8 March 2024

Atmospheric Measurement Techniques Discussions

surface temperature, leading to large uncertainties in climate change projections (Forster et al., 2021; Sassen et al., 2007; Watanabe and Zelinka, 2019). Grasping the variations in cloud properties is crucial for a comprehensive understanding of cloud dynamics and their radiative impacts on global climate change. The advancement of science and technology has positioned satellite remote sensing as a pivotal tool for monitoring cloud behaviors across diverse spatial and temporal scales. Active satellites like CloudSat and CALIPSO (Cloud-Aerosol Lidar and Infrared Pathfinder Satellite Observations) offer unparalleled cloud profiling capabilities (Marchand et al., 2008; Sassen et al., 2009). Conversely passive satellites, renowned for their extensive swath observations, are widely applied in a range of atmospheric research.

In recent decades, numerous efforts have been made to retrieve cloud properties using passive satellite instruments (Lai et al., 2019; Li et al.,2023; Min et al., 2020; Minnis et al., 2011; Poulsen et al., 2012; Shi et al.,2019; Tan et al., 2022; Zhao et al., 2012). A common method involves combining data from visible (VIS) and near-infrared (NIR) channels to construct lookup tables (LUT) for daytime cloud microphysical properties, such as cloud optical thickness (COT) and cloud effective radius (CER) (Painemal and Zuidema, 2011; Twomey et al., 1980; Nakajima et al., 1990). This approach is grounded in the principle that cloud reflectance in non-absorbing VIS wavelengths predominantly signifies COT, while reflectance in absorbing NIR wavelengths is closely related to cloud effective radius (Arking and Childs, 1985; Rossow et al., 1989). Additionally, distinguishing liquid water from ice clouds using NIR channels (e.g., 1.65 μm) have also proven beneficial for deriving cloud top height (CTH) (Harshvardhan et al., 2009; Häkansson et al., 2018; Menzel et al., 2008). Nonetheless, these VIS/NIR-based methodologies are confined to daytime operations owing to their reliance on incident solar radiation, absent during nighttime hours.

Alternatively, night-time cloud properties can be retrieved using thermal infrared (TIR) radiometry from passive satellite. Inoue (1985) employed the split-window method, leveraging brightness temperature (BT) and BT differences across various window channels, to derive COT and CER. Subsequently, numerous improvements and enhancements have been made to this method (Hamada and Nishi, 2010; IWABUCHI et al., 2018; Yang et al., 2005). Wang et al. (2016a) implemented an optimal estimation-based (OE) algorithm with Moderate Resolution Imaging Spectroradiometer (MODIS) infrared (IR) observations for cloud property retrieval, demonstrating the suitability of IR channels for

https://doi.org/10.5194/amt-2024-36
Preprint. Discussion started: 8 March 2024

Atmospheric Measurement Techniques Discussions

thin ice cloud properties during both daytime and nighttime (Wang et al., 2016b). In addition, the CO_2-slicing method, which utilizes adjacent ~15 μm CO_2 absorption channels, is able to retrieve CTH effectively (Smith et al., 1974; Menzel et al., 1983). The atmospheric window IR measurements, such as at 11 μm, are also useful for CTH determination by comparing with the ambient atmospheric temperature profile (Garrett et al., 2009; Hong et al., 2007). However, IR window methods are less effective for optically thick clouds as their BT nears asymptotic values (Garrett et al., 2009; Iwabuchi et al., 2016). While far infrared channels are useful for clouds with substantial optical thickness (Libois et al., 2017), their limited presence on most current satellites limits their application. Moreover, the retrieval methods based on plane-parallel cloud radiative transfer (RT) models face global application challenges due to their high computational demands (Wang et al., 2013).

Recently, machine learning techniques such as random forests, artificial neural network, and deep learning have gained significant traction in remote sensing (Bai et al., 2021; Guo et al. 2022; Shi et al.,2020; Tan et al.,2023; Yuan et al., 2020; Zhao et al., 2023). Häkansson et al. (2018) used a neural network algorithm to retrieve cloud top properties from several passive polar orbit sensors, greatly improving CTH retrievals. Advanced machine learning algorithms have particularly enhanced CTH retrievals for high and thin clouds (Min et al., 2020). Wang et al. (2022) developed a CNN-based framework (TIR-CNN), utilizing TIR radiometry from MODIS to retrieve COT, CER, and CTH. This method demonstrates satisfactory performance compared to both passive and active cloud products and is effective during both daytime and nighttime(Wang et al., 2022, 2023). Tana et al. (2023) obtained cloud detection and cloud microphysical properties with high spatial-temporal resolutions from TIR spectral channels of Himawari-8 using a machine learning algorithm. Zhao et al. (2023) applied a deep-learning ResUnet model for retrieving cloud phase (CLP), COT, CER, and CTH using FY4A satellite observations.

However, the reliance of these machine learning methods on mathematical and statistical approaches typically leads to an implicit assimilation of the relationships between cloud properties and radiance observations, lacking direct physical interpretation. A great number of cloud property users favor remote sensing products that offer explicit physical interpretations. Therefore, enhancing traditional inversion algorithms with machine learning algorithms can be beneficial.

https://doi.org/10.5194/amt-2024-36
Preprint. Discussion started: 8 March 2024

Atmospheric Measurement Techniques Discussions

In this study, we integrate traditional radiative transfer simulations with TIR-CNN retrievals using the OE method (OE-CNN-IR) to retrieve COT, CER, and CTH from MODIS, which is effective under both daytime and nighttime conditions. The Community Radiative Transfer Model (CRTM) is utilized to simulate MODIS IR observations and generating LUT for cloud properties. The TIR-CNN retrievals are employed as initial prior states, followed by an iterative optimization to refine these retrievals. The performance of the proposed OE-CNN-IR model is subsequently compared with a traditional OE method utilizing fixed priori states. Details of the data and the enhanced OE-CNN-IR method are presented in Section 2. Section 3 outlines the retrieval results and their evaluation against passive and active cloud products. Conclusions are summarized in Section 4.

2 Data and Methodology

2.1 Data

2.1.1 MODIS data

This study utilizes global data observed by MODIS instrument on the Aqua spacecraft. Aqua-MODIS continuously monitors the earth-atmosphere system with 36 spectral bands ranging from 0.405 to 14.385 μm. For this research, the Aqua-MODIS official Collection 6.1 (C6.1) products (MYD021KM, MYD03, MYD35, MYD06 and MCD12C1), available at https://ladsweb.modaps.eosdis.nasa.gov/search/, have been selected for this study. These products, with spatial resolution of 1km and 5km, are chosen for their widely accepted quality (Wang and Christopher, 2003). In this study, the TIR radiations from Aqua-MODIS collection 6.1 (C6.1) Level 1B calibrated radiances products (MYD021KM) are converted to BTs using the Planck function. Additionally, atmospheric parameters from MYD03 and MYD06, including surface temperature, land surface type, and cloud phase, are used as ancillary data for LUT construction and forward radiative simulations. Cloud optical and physical parameters such as COT, CER and CTH from MYD06 serve to verify the accuracy of daytime retrievals. All parameters are aligned to a 5-kilometer spatial resolution grid, ensuring data and variable consistency. To validate the universality of the inversion algorithm, retrievals are conducted using data from one representative day each month in 2009, capturing the variability of atmospheric conditions throughout the year and facilitating a comprehensive evaluation across different scenarios. By selecting days representative of each month, we

https://doi.org/10.5194/amt-2024-36
Preprint. Discussion started: 8 March 2024


Atmospheric Measurement Techniques Discussions

aim to assess the algorithm's performance under varying seasonal and weather patterns. Table 1 summarizes the data and parameters used in our retrieval model.

2.1.2 Active Lidar Detection cloud products

CALIOP, a space-based lidar instrument onboard the CALIPSO satellite, provides vertical profiles of clouds and aerosols in Earth's atmosphere. CALIOP can perform observations at both daytime and nighttime, overcoming the limitations of passive optical instruments, but it could not penetrate thick clouds. The Cloud Profiling Radar (CPR) aboard the CloudSat satellite is a radar system that sends out microwave pulses and measures the reflected energy from clouds. This technique is particularly adept at determining the structure and ice content within clouds, but fails to detect thin clouds. The DARDAR product (Delanoe and Hogan, 2010), integrating data from both CALIOP and CPR, offers comprehensive atmospheric column view that neither instrument can achieve independently. This extensive dataset includes information on cloud top and base heights, optical thickness, ice content, and aerosol layers. In our study, the ice cloud product of DARDAR is used to evaluate the inversion results during both daytime and nighttime conditions.

Table 1. Summary of MODIS data sources and preprocessing parameters.

Product name	Spatial Resolution	Variables	Unit
MYD021KM	1 km	Band 27	W/ (m^2 μm sr)
		Band 28	W/ (m^2 μm sr)
		Band 29	W/ (m^2 μm sr)
		Band 31	W/ (m^2 μm sr)
		Band 32	W/ (m^2 μm sr)
		Band 33	W/ (m^2 μm sr)
		Band 34	W/ (m^2 μm sr)
		Band 35	W/ (m^2 μm sr)
		Band 36	W/ (m^2 μm sr)
MYD03	1 km	Sensor Zenith	°
		Land/Sea Mask	-
MYD06	1km	Cloud Effective Radius	μm

https://doi.org/10.5194/amt-2024-36
Preprint. Discussion started: 8 March 2024

Atmospheric Measurement Techniques Discussions

		Cloud Optical Thickness	-
		Cloud water path	Kg/m^2
		Cloud Phase Optical Properties	-
	5km	Cloud Phase Infrared	-
		Cloud Top Pressure	hPa
		Surface Temperature	K

2.2 Development of the retrieval algorithm

Figure 1 illustrates the architecture of our retrieval models. Initially, atmospheric parameters including temperature, humidity and ozone from the Fifth Generation of the European Centre for Medium-Range Weather Forecasts (ECMWF) Reanalysis (ERA5) are used to construct lookup tables for each 0.25°x0.25° spatial grid box. These LUTs enumerate the BT for each channel corresponding to varying COT, CTH and CER. Subsequently, the OE method is performed to retrieve cloud properties. In this approach, the TIR-CNN derived cloud properties provide the initial estimate, which is subsequently refined through iterative minimization of the objective cost function. This method iteratively adjusts parameters to reconcile observed data with model predictions. Further details are presented below.

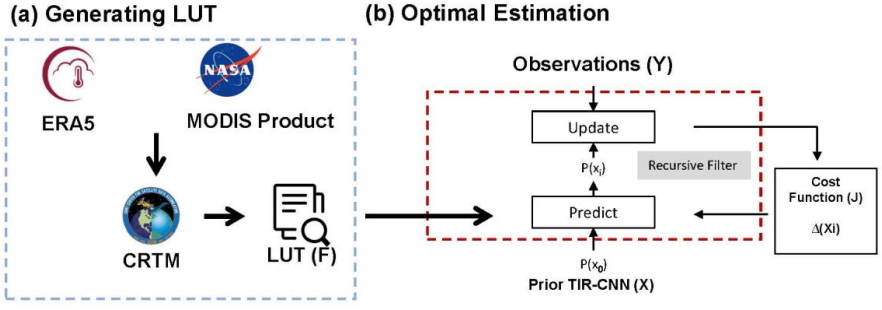

Figure 1. The architecture of the retrieval model. (a) The establishment of look-up table. (b) The iteration steps in the optimal estimation progress.

2.2.1 Forward Model

The CRTM, developed by the U.S. Joint Center for Satellite Data Assimilation (JCSDA), spans a broad spectrum of channels from visible to microwave. It is widely used in simulating radiances (and Jacobians) at the top of the atmosphere for various satellite sensors, owing to its flexible interface, sophisticated

https://doi.org/10.5194/amt-2024-36
Preprint. Discussion started: 8 March 2024

Atmospheric Measurement Techniques Discussions

radiative transfer processes, and efficient numerical computation(Han et al., 2006). The model divides the atmosphere into a series of vertical layers, and the temperature, pressure and composition of each layer is assumed to be homogenous. CRTM solves the radiative transfer equations throughout the atmosphere, and is able to simulates the radiances observed by satellites. Its precision and reliability have been extensively corroborated by ground-based and satellite observations(Zou et al., 2016). For each grid cell, the CRTM simulates TIR radiances corresponding to various COT, CER, and CTH values at each location, from which a LUT is subsequently constructed. Table 2 provide a detailed list of the cloud properties and ancillary parameters used in these calculations.

Table 2. Goemetries and cloud properties selected to calculate the cloud lookup tables

	Variable Names	Notes
Reference cloud properties	COT	0.01, 0.03, 0.05, 0.10, 0.20, 0.30, 0.40, 0.50, 0.60, 0.70, 0.80, 0.90, 1.00, 1.20, 1.40, 1.60, 1.80, 2.00, 2.50, 3.00, 3.50, 4.00, 4.50, 5.00, 5.50, 6.00, 6.50, 7.00, 7.50, 8.00, 8.50, 9.00, 9.50, 10.0, 12.0, 15.0, 20.0, 25.0, 30.0, 50.0
	CER(μm)	5, 10, 15, 20, 25, 30, 35, 40, 45, 50, 55, 60, 65, 70, 75, 80, 85, 90
	CTH(km)	0.1,0.8,1.15,1.5,2,2.5,3.5,5,6.25,8,10,12,14,16
Model parameter	Surface temperature(K)	MYD06
	Land type	MCD12C1, IGBP
	Cloud type	MYD06, Cloud Phase
	Temperature profile(K)	ERA5, Temperature
	Water vapor profile(g/kg)	ERA5, Specific humidity
	Ozone profile(g/kg)	ERA5, Ozone mass mixing ratio

https://doi.org/10.5194/amt-2024-36
Preprint. Discussion started: 8 March 2024


Atmospheric Measurement Techniques Discussions

The outputs of the forward model can be expressed as a function of cloud properties and ancillary parameters:

$$Y = [BT_1 BT, BT_2, \dots\dots, BT_m]^T = F[X(COT, CER, CTH), P] + e, \quad (1)$$

where Y is a vector consisting of m MODIS IR observations in BT, P is a vector encompassing various ancillary variables, including air temperature, water vapor concentration, ozone concentration profiles, surface emissivity spectrum, and surface temperature, and e is an error term. For the retrieval process, several Jacobian matrices are required. The matrix $K_{F/X}$ with dimensions m×m consists of partial derivatives of *m* MODIS IR observations with respect to *n* cloud parameters:

$$K_{F/X} = \left[\frac{\partial F}{\partial COT}, \frac{\partial F}{\partial CER}, \frac{\partial F}{\partial CTH}\right]^T, \quad (2)$$

Figure 2 depicts the variation in CRTM output (F) (expressed in BT) as a function of ice cloud properties, derived from a simulation using the atmospheric profile dated June 10, 2009, at 00:00 UTC, at coordinates 175.87°E longitude and 60.55°N latitude. With fixed CER and CTH, the TOA BTs in MODIS IR bands generally decrease with increasing COT. Notably, for COT>10, the slopes approach zero, causing challenges in inversion accuracy. In the case of fixed COT and CTH, TOA BTs decrease with increasing CER values when CER is below 10 μm across all channels, followed by minor oscillations in most channels, except that band 29 shows significant variations. For CTH values under 11 km, TOA BTs is negatively correlated with CTH noticeably.

Figure 3 shows the relationship between TOA BTs and liquid cloud properties, which reveals a weaker response to changes in COT and CER compared to ice clouds. Nevertheless, TOA BTs decreases noticeably with increasing water cloud CTH. In summary, CTH is the most accurately determinable variable for both ice and water clouds due to the high sensitivity of TOA BTs to CTH. For ice clouds, COT values below 10 generally allow for more accurate retrieval of cloud properties in theory. However, retrieving CER for ice clouds poses greater challenges due to the complexity of ice particle size distribution and shape. Water clouds, conversely, show no strong sensitivity of TOA BTs to both COT and CER, and it is more difficult to accurately retrieve these cloud properties solely based on TOA BT observations.

https://doi.org/10.5194/amt-2024-36
Preprint. Discussion started: 8 March 2024

Atmospheric Measurement Techniques Discussions

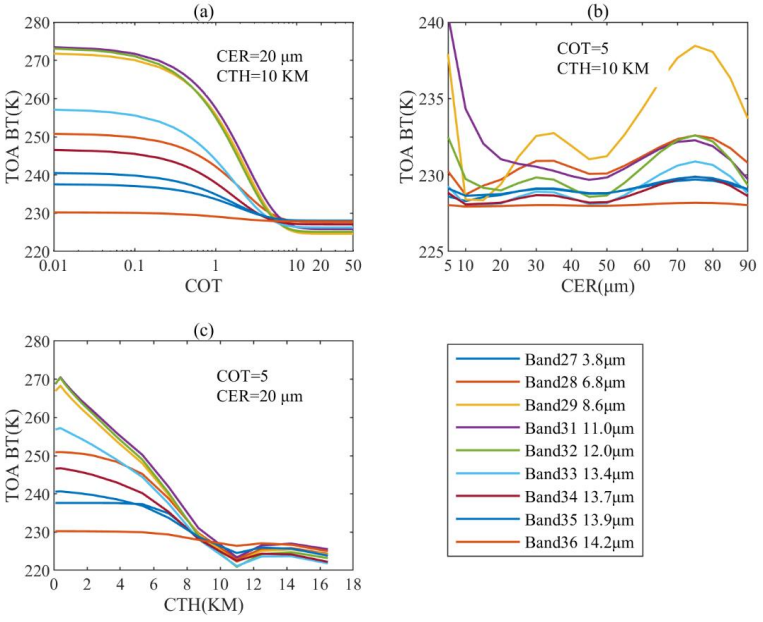

180

Figure 2. Radiative transfer model simulations for ice clouds. The atmospheric profile is from the coordinates with a longitude of 175.87°E and a latitude of 60.55°N, on June 10, 2009, at 00:00 UTC. (a) TOA BTs as a function of COT, when CER and CTH is set to 20 μm and 10 km, respectively. (b) BT as a function of CER, when COT and CTH is set to 5 and 10km, respectively. (c) BT as a function of CTH, when COT and CER is
185 **set to 5 and 20 μm, respectively.**

https://doi.org/10.5194/amt-2024-36
Preprint. Discussion started: 8 March 2024

Atmospheric Measurement Techniques Discussions

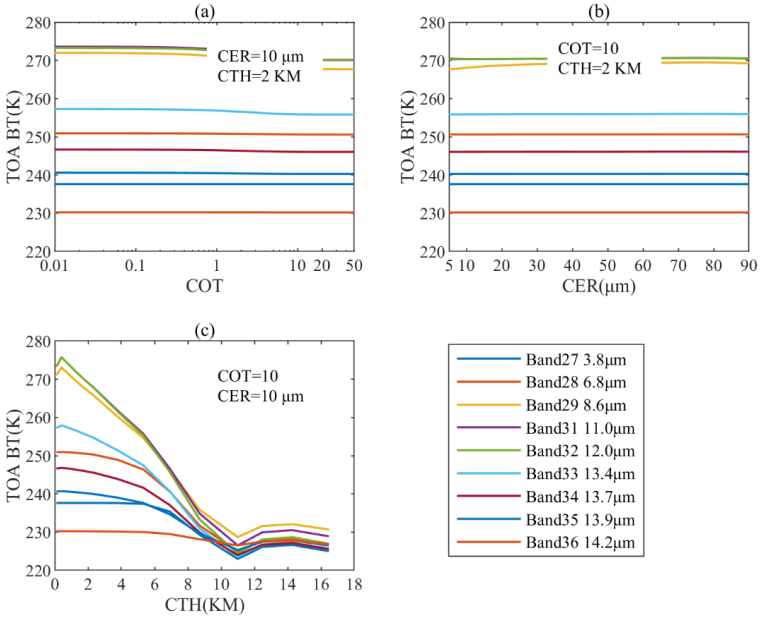

Figure 3. Same as Fig. 2, but for liquid clouds.

2.2.2 Optimal Estimation-Based Retrieval Method

The OE-based retrieval method, as introduced by (Rodgers, 2000), is designed to derive the best estimates of atmospheric quantities (such as temperature, humidity, aerosol concentration, or trace gas concentrations) by minimizing the discrepancy between observed measurements and the model predictions. This method combines information from both the measurement data and a priori knowledge, typically obtained from atmospheric models or ancillary data sources. A key strength of the OE method is its proficiency in addressing complex atmospheric retrieval challenges, enabling simultaneous retrieval of multiple parameters in contexts where physical processes are nonlinear and highly coupled. Additionally, it provides a rigorous and statistically robust method to estimate atmospheric parameters, along with quantifying the associated uncertainties.

The OE method aims to identify the most probable state variables by minimizing a cost function J:

$$J = [F(X,P) - Y]^T S_y^{-1}[F(X,P) - Y] + [X - Xa]^T S_a^{-1}[X - X_a], \quad (3)$$

where X_a and X are the priori and posterior state vectors, respectively. S_y and S are the covariance matrices of the observation-to-simulation differences and the uncertainty of the priori state vector,

https://doi.org/10.5194/amt-2024-36
Preprint. Discussion started: 8 March 2024

Atmospheric Measurement Techniques Discussions

respectively. Then we employ an iterative process to find an optimal solution based on observed data and prior information. Mathematically, the iterative process for *(i+1)*'th iteration is encapsulated by:

$$X_{i+1} = X_i + \left(K_{F/X,i}^T S_{y,i}^{-1} K_{F/X,i} + \gamma_i I\right)^{-1} K_{F/X,i}[Y - F(X_i)], \quad (4)$$

where γ is a positive damping parameter, which plays a crucial role in controlling the convergence behavior of the algorithm. The value of γ varies with each iteration based on the variation of the cost function *J*. Typically, γ initially is set to a positive constant, such as 0.01. During each iteration, the cost function is evaluated. If the new cost function is smaller than that of the previous iteration, γ is decreased by a factor of 5. Conversely, if the cost function increases, γ is increased by the same factor. As the value of γ approaches 0, Eq. 4 approximates the Gauss-Newton method. Alternatively, when γ approaches a large value, Eq. 4 begins to resemble the gradient descent method, which iteratively adjusts the estimated state variables opposite to the gradient of the cost function. By dynamically adjusting γ based on the changes of the cost function, the OE retrieval algorithm balances the efficiency of the Gauss-Newton method and the robustness of the gradient descent method. This adaptive adjustment of γ enables the algorithm to adapt to the local curvature of the cost function, enabling a more effective convergence to the optimal solution.

2.3 Metrics for performance evaluation

In this study, the magnitude of forecast errors, systematic bias errors, and linear correlation between outputs and standard values are quantitatively assessed using three key statistical metrics: root mean squared error (RMSE), mean bias error (MBE), and the Pearson correlation coefficient (r).

$$RMSE = \sqrt{\frac{\sum_{i=1}^{N}(y_i - f_i)^2}{N}}, \quad (5)$$

$$MBE = \frac{\sum_{i=1}^{N} f_i - y_i}{N}, \quad (6)$$

$$r = \frac{\sum_{i=1}^{N}(f_i - \bar{f})(y_i - \bar{y})}{\sqrt{\left(\sum_{i=1}^{N}(f_i - \bar{f})^2\right)\left(\sum_{i=1}^{N}(y_i - \bar{y})^2\right)}}, \quad (7)$$

where N is the total number of calculated points, y and f are the true and estimated values, respectively.

https://doi.org/10.5194/amt-2024-36
Preprint. Discussion started: 8 March 2024

Atmospheric Measurement Techniques Discussions

3 Results and discussion

3.1 Case studies of OE-CNN-IR and OE-IR retrievals

To illustrate the daytime efficacy of the proposed method, a granule from Aqua-MODIS, captured at 03:00 UTC on June 10, 2009, has been chosen. This particular granule spans the southwestern Pacific Ocean, encompassing the geographical region from 0° to 20°S latitude and from 150°E to 175°E longitude, as depicted in Fig. 5. Figure 4 compares observed BT with those derived from CRTM. Figures 4(a-c) show CRTM-simulated radiances using baseline MODIS cloud products, serving as a control scenario for comparative analysis. The correlation coefficients for channels 29, 31, and 32 are 0.877,0.905 and 0.891, respectively, indicating CRTM's proficiency in simulating MODIS cloud products. However, there is a persistent negative MBE across these channels. Figures 4(d-f) present a comparison between observations and BT simulated by CRTM and TIR-CNN retrievals, with outcomes that are analogous to those depicted in Figs. 4(a-c). The pronounced correlation indicates that CNN-based inputs proficiently replicate the spatial and radiometric features of clouds, showing high consistency with MODIS MYD06 products. When OE-CNN-IR or OE-IR cloud property retrievals are used to simulate BT, the correlation coefficients between the simulated BT and observations increases significantly, and the absolute values of MBE and RMSE decreases significantly (as shown in Figs. 4g-l). The improvement is attributed to the OE iterations, which reduce the discrepancy between simulated and observed BT. The results indicate that retrievals of the OE-CNN-IR methods align more closely with BT observations compared to the stand-alone TIR-CNN model.

https://doi.org/10.5194/amt-2024-36
Preprint. Discussion started: 8 March 2024

Atmospheric Measurement Techniques Discussions

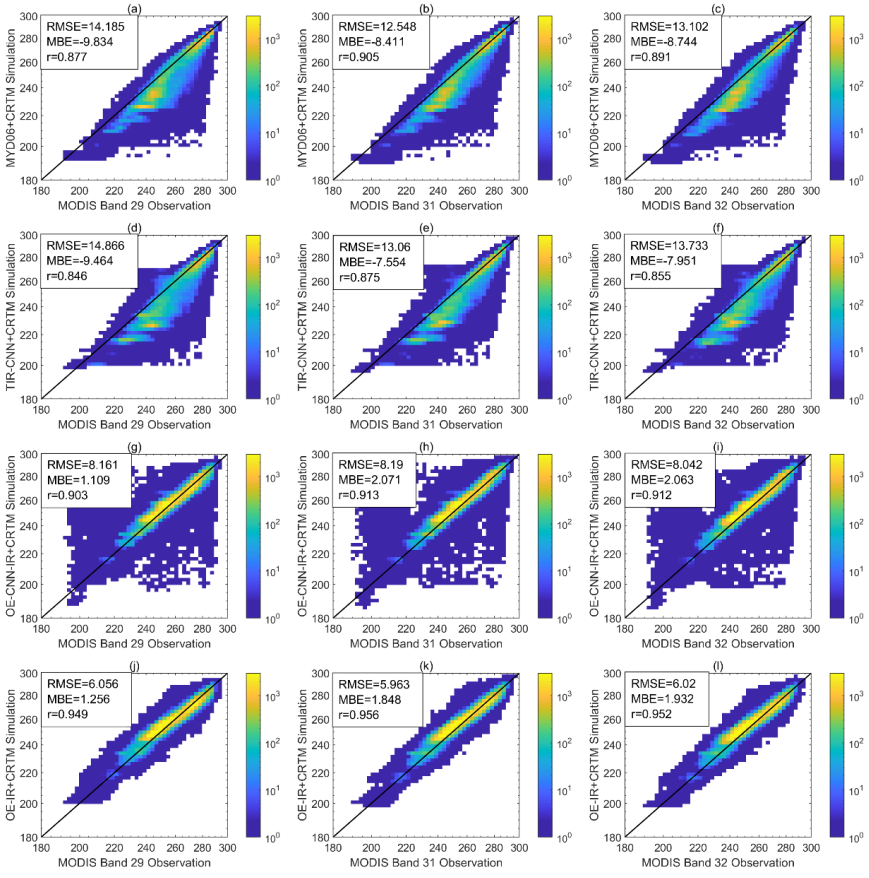

Figure 4. Comparison between MODIS BT observations and simulated BT based on MODIS cloud properties (upper), TIR-CNN initial inputs (middle), OE-CNN-IR estimations (lower) and OE-IR estimations(bottom), based on an illustrative granule of 10 June 2009 (Fig. 5). The first column is the comparison between the simulation and observation of band 29, the middle column is for band 31, and the right column is for band 32.

Figures 5 (a-c) show the spatial distribution of BT for each respective channel. These measurements reveal variations in thermal radiation, which correlated with cloud properties specific to the wavelengths of the channels used. Figures 5(d-f) show the cloud physical properties as derived using standard MODIS retrieval algorithms. The COT, CER, and CTH from the MYD06 product provide a benchmark for comparison with other inversion methods. The analysis of BT from channels 29, 31, and 32 shows a clear negative correlation with both COT and CTH, and regions with higher BT typically correspond to clouds with smaller optical thickness and lower cloud top heights. This is in line with the principle that thinner clouds permit more infrared radiation to escape from the Earth's surface and atmosphere, leading to

https://doi.org/10.5194/amt-2024-36
Preprint. Discussion started: 8 March 2024


Atmospheric Measurement Techniques Discussions

higher observed BT. Furthermore, the analysis indicates that clouds with higher BT generally have lower altitudes. The patterns in Fig. 5, which display cloud properties derived from various inversion techniques, corroborate the physical relationships illustrated in Figs. 2 and 3. These results support the hypothesis that BT can serve as effective proxies for key cloud properties like COT and CTH, essential for comprehending cloud dynamics and their effects on weather and climate systems. Figures 5 (g-i) present the retrieval results from the deep learning algorithm TIR-CNN method. The CNN-derived retrievals are not only consistent with MYD06 products in spatial patterns, but also agree well with the magnitudes of results. Figures 5 (j-l) present the retrieval results from the OE-CNN-IR method, showing similar spatial distributions to the standard MYD06 products for COT and CTH. However, significant differences are noted in CER retrieved by OE-CNN-IR and MYD06 products, which is consistent with Wang et al. (2016), which highlighted substantial discrepancies in CER retrieved using OE-IR and VNIR/SWIR/MWIR methods.

Figures 5 (m-o) show the results retrieved using the traditional OE-IR method with climatological priori states, which employs climatological values of COT, CER and CTH as initial guesses for OE iteration. In case where COT values are below a certain threshold, the OE-IR COT closely match MYD06 products, indicating that it is able to capture the COT of thinner clouds. However, the inability of OE-IR to retrieve COT values greater than 10 suggests a limitation in the technique's sensitivity to optically thicker clouds, aligning with findings from Wang et al. (2016). This threshold effect arises from the TIR BT independence to COT in thick clouds (as shown in Fig. 2a). The performance of CER and CTH retrievals using the OE-IR method is comparable to that of the OE-CNN-IR method.

https://doi.org/10.5194/amt-2024-36
Preprint. Discussion started: 8 March 2024

Atmospheric Measurement Techniques Discussions

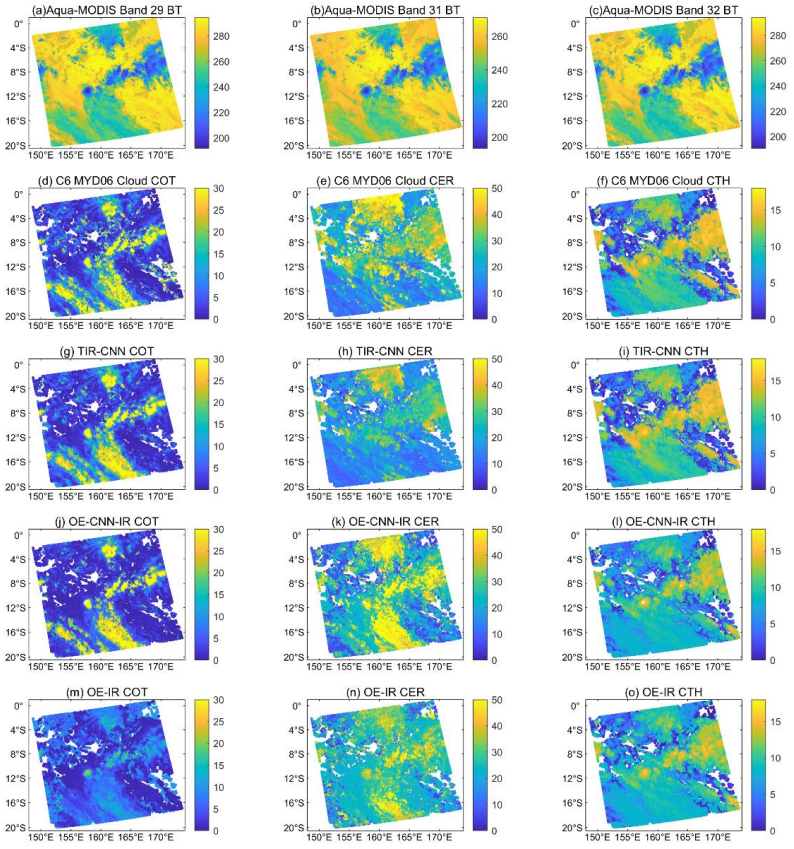

Figure 5. Comparison of cloud properties obtained from the OE-CNN-IR model, OE-IR model and standard MODIS products for an illustrative daytime granule on 10 June. 2009 (03:00 UTC). (a, b, c) are BT image of MODIS band 29,31 and 32, respectively. (d, e, f) are the COT, CER, and CTH from the MYD06 product, respectively. (g, h, i) are the COT, CER, and CTH from the CNN-IR model, respectively. (j, k, l) are the COT, CER, and CTH from the OE-CNN-IR model, respectively. (m, n, o) are the COT, CER, and CTH from the OE-IR model, respectively.

Fig. 6 illustrates a nighttime case of cloud parameter retrievals using CNN-IR, OE-CNN-IR and OE-IR methods. The data for this analysis is sourced from a randomly selected granule captured on February 10th, 2009, at 21:00 UTC. Figs. 6(a-c) display the BTs at channels 29, 31, and 32, and Figs. 6(d-f) shows the COT, CER, and CTH retrieved by the TIR-CNN algorithm. The relationship between COT and CTH with BT at night is generally consistent with that during the day. Figs. 6(g-i) shows the COT, CER, and CTH retrieved by the OE-CNN-IR algorithm. The OE-CNN-IR retrievals align well with the high and low-value areas in the BT images, indicating that OE-CNN-IR effectively discerns the

https://doi.org/10.5194/amt-2024-36
Preprint. Discussion started: 8 March 2024

Atmospheric Measurement Techniques Discussions

intricate spatial variations in cloud properties during nighttime conditions. Figs. 6(j-l) display the cloud parameters retrieved using the OE-IR method. In this analysis, the predominance of values falls below 10, which signifies a more constrained retrieval scope when contrasted with the OE-CNN-IR method. Nevertheless, the distribution of CTH derived from OE-IR closely mirrors that obtained from OE-CNN-IR, affirming its dependability for estimating the vertical extent of clouds. Additionally, both methods exhibit comparable distributions in CER.

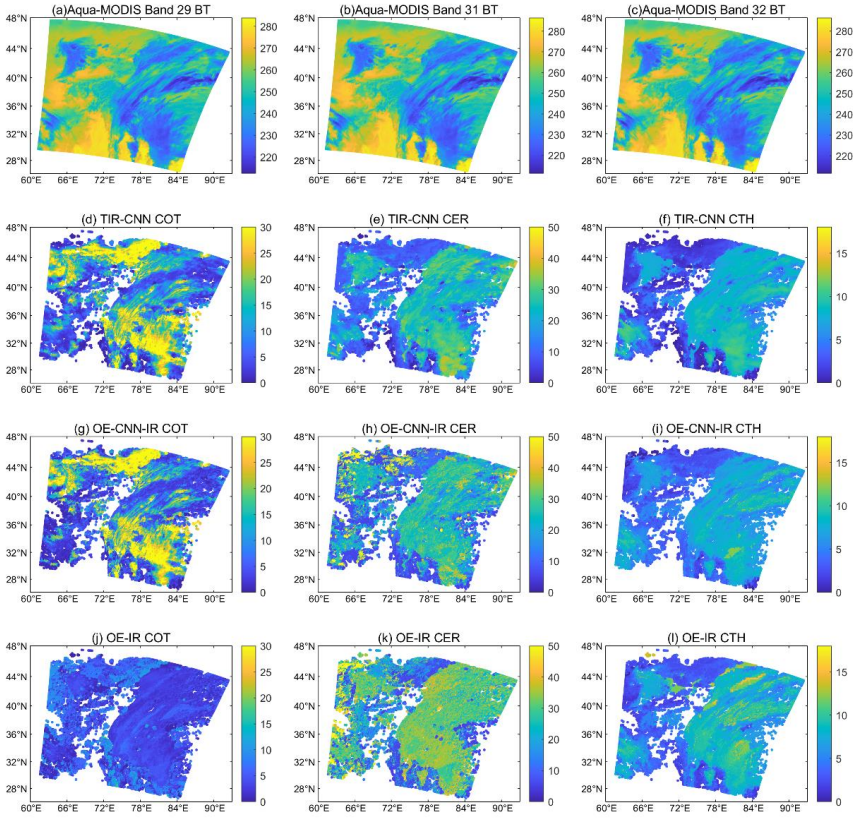

Figure 6. Comparison of cloud properties obtained from the OE model and standard MODIS products for an illustrative nighttime granule on 10 February 2009 (21:00 UTC). (a) BT image of MODIS band 29. (b) BT image of MODIS band 31. (c) BT image of MODIS band 32. (d, e, f) are the COT, CER, and CTH from the TIR-CNN, respectively. (g, h, i) are the COT, CER, and CTH from the OE-CNN-IR model, respectively. (j, k, l) are the COT, CER, and CTH from the OE-IR model, respectively.

https://doi.org/10.5194/amt-2024-36
Preprint. Discussion started: 8 March 2024

3.2 Comparison between retrievals and MYD06 products in the daytime

Figure 7 presents scatterplots that provides pixel-level comparisons of cloud property retrievals from OE-CNN-IR and OE-IR against the MYD06 ice cloud products over ocean for 2009. The left column of Fig. 7 offers a detailed pixel-by-pixel comparison for COT, CER, and CTH between OE-CNN-IR and the MYD06 ice cloud products. The right column displays comparisons between MYD06 cloud products and OE-IR retrievals. The color scale in these plots indicates the number of observations in each grid, visually representing data point density. Retrieval constraints, including a limit on Solar Zenith Angles (SZA) to less than 60 degrees and latitudes between 60°S and 60°N, ensure consistency and reliability in these comparisons. In Fig.7(a), the correlation coefficient between OE-CNN-IR COT and MYD06 COT is 0.784 for all clouds, indicating a strong positive correlation. In comparison, OE-IR achieves a COT correlation coefficient of 0.66 against MODIS products for all clouds, indicating a slightly weaker relationship than that reported in Wang et al. (2016). Both OE-CNN-IR and OE-IR show consistent performance for COT below 10, but OE-CNN-IR performs much better for thicker clouds. With respect to CER, both algorithms demonstrate moderate to weak correlation coefficients, reflecting the inherent physical constraints of the retrieval process. Nonetheless, OE-CNN-IR outperforms OE-IR with a correlation coefficient of 0.517, suggesting enhanced performance. For CTH retrieval, both OE-CNN-IR and OE-IR demonstrate good performance, with correlation coefficients of 0.846 and 0.792, respectively. Overall, the statistical analysis in Fig. 7 underscores the superior retrieval capability of OE-CNN-IR, particularly for COT, compared to OE-IR.

Figure 8 expands the ice cloud analysis from Fig. 7 to encompass all types of clouds over both land and ocean, offering a more comprehensive evaluation of the retrieval algorithms across varied cloud conditions. In the case of thick water clouds, the BT is not sensitive to COT, leading to most OE-IR COT retrievals clustering around the initial value of 10. This indicates difficulties in effectively retrieving COT for water clouds, so the OE-IR method has been used to retrieve cloud properties of ice clouds only. In contrast, the performance of OE-CNN-IR is much better. This enhanced capability is credited to OE-CNN-IR's effective estimation of initial values, allowing for accurate retrievals even in situation of lower BT sensitivity, as observed in water clouds. Regarding CER, the gradient of CER with respect to BT of water clouds tends toward zero. This induces numerous striping artifacts along the edges of each lookup tables used in the retrieval process. These artifacts signal the limitations of the retrieval algorithm under

https://doi.org/10.5194/amt-2024-36
Preprint. Discussion started: 8 March 2024

minimal BT gradient conditions. Despite these challenges for CER, both OE-CNN-IR and OE-IR perform exceptionally well in retrieving CTH, with r of 0.917 and 0.921, respectively. These high correlations reflect the algorithms' effectiveness in estimating CTH. The success of both OE-CNN-IR and OE-IR in CTH retrievals highlights the importance of well-defined physical mechanisms in the OE retrieval process. This illustrates that precise retrieval of cloud properties, which is vital for atmospheric modeling and climate research, can be realized when the underlying physical mechanisms are thoroughly represented and comprehended.

https://doi.org/10.5194/amt-2024-36
Preprint. Discussion started: 8 March 2024

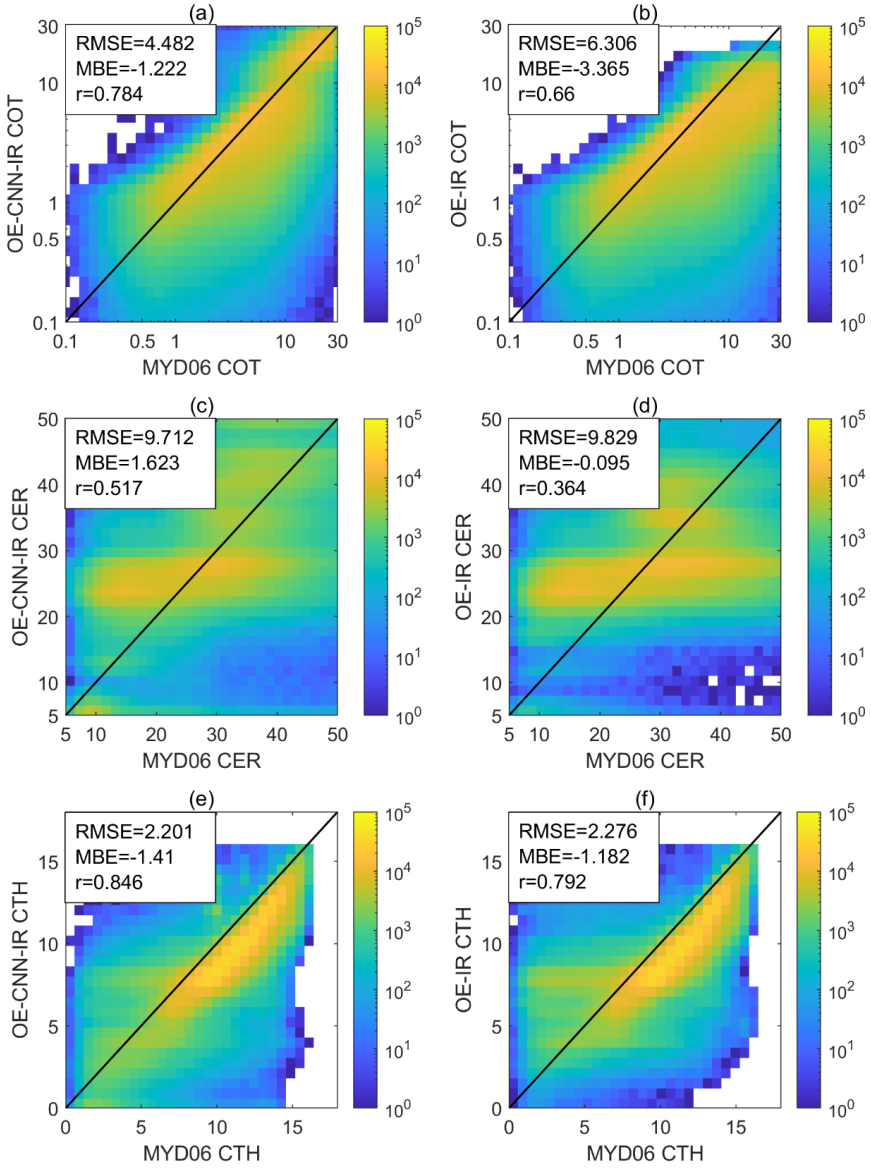

Figure 7. Scatterplots of the pixel level comparisons between the retrievals and MYD06 products for ice clouds over oceans. (left column) Pixel-by-pixel comparisons of COT, CER, and CTH from OE-CNN-IR with the MYD06 ice cloud products over ocean in 2009. (right column) Scatterplots of the pixel level comparisons between the MYD06 cloud products and OE-IR comparable retrievals. Color shadings denote the number of observations in each respective pixel. All comparable retrievals are constrained to cases with SZA < 60° and latitude between 60°S and 60°N.

https://doi.org/10.5194/amt-2024-36
Preprint. Discussion started: 8 March 2024

Atmospheric Measurement Techniques Discussions

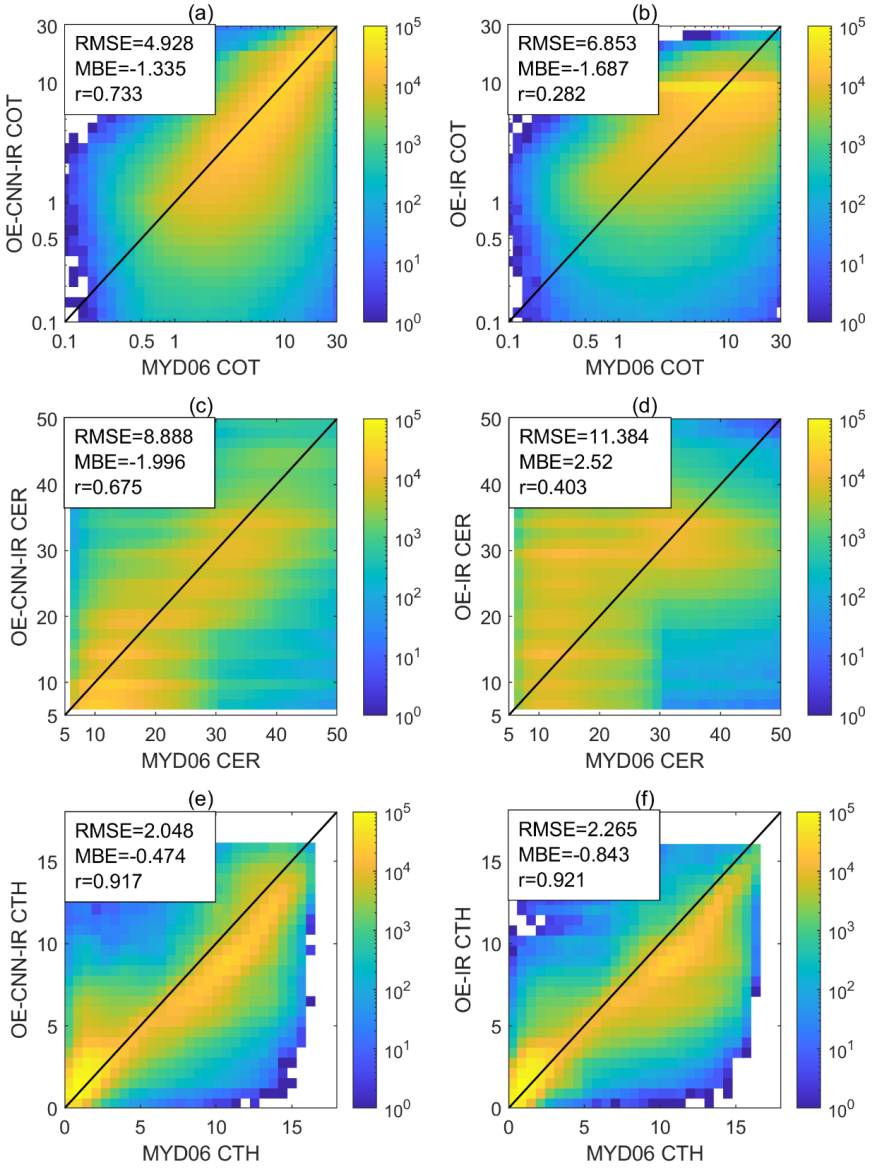

Figure 8. Same as Fig. 7, but includes liquid clouds over ocean, and all clouds over land.

3.3 Comparison with products from active sensors

Under nighttime conditions, where standard MYD06 cloud products do not offer cloud optical properties, the evaluation is supplemented by incorporating near-real-time data from active sensors.(DARDAR, derived from CloudSat/CALIPSO observations). To align with MODIS observations, single-layer

https://doi.org/10.5194/amt-2024-36
Preprint. Discussion started: 8 March 2024


Atmospheric Measurement Techniques Discussions

measurements from CALIPSO are spatially matched by restricting their distance to less than 333 meters, the distance between adjacent CALIPSO footprints. Additionally, the temporal difference is restricted to under 90 seconds. Spatially and temporally co-located samples from 2009 are employed to evaluate the performance and generalization capabilities of the OE model during night conditions. These criteria are applied to achieve the closest possible data correspondence between the two different instruments, facilitating a meaningful assessment of the OE model's nighttime performance.

Figure 9 presents a detailed comparison of COT retrievals for ice clouds using OE-CNN-IR and OE-IR methods, benchmarked against DARDAR cloud products. The comparisons are confined to latitudes between 60°N and 60°S to ensure a comprehensive assessment across both daytime and nighttime conditions. The daytime correlation coefficient for OE-CNN-IR versus DARDAR COT is 0.615, with slightly lower nighttime correlation of 0.537. These values suggest a moderate concordance of OE-CNN-IR with DARDAR, notably in the context of the challenges involved in accurately retrieving COT for ice clouds. In contrast, OE-IR exhibits substantially lower correlation coefficients, with 0.383 during the day and 0.289 at night. Notably, the OE-CNN-IR method demonstrate higher correlations for COT > 10, indicating enhanced accuracy in these ranges. This suggests that OE-CNN-IR is more adept at capturing the variability of thicker ice clouds, which is crucial for understanding cloud radiative effects and their implications for weather and climate systems. The comparisons in Fig. 9 highlight the improved performance of OE-CNN-IR over OE-IR in capturing cloud properties throughout the diurnal cycle, positioning it as a potentially more reliable tool for cloud characterization under diverse illumination conditions.

https://doi.org/10.5194/amt-2024-36
Preprint. Discussion started: 8 March 2024

Atmospheric Measurement Techniques Discussions

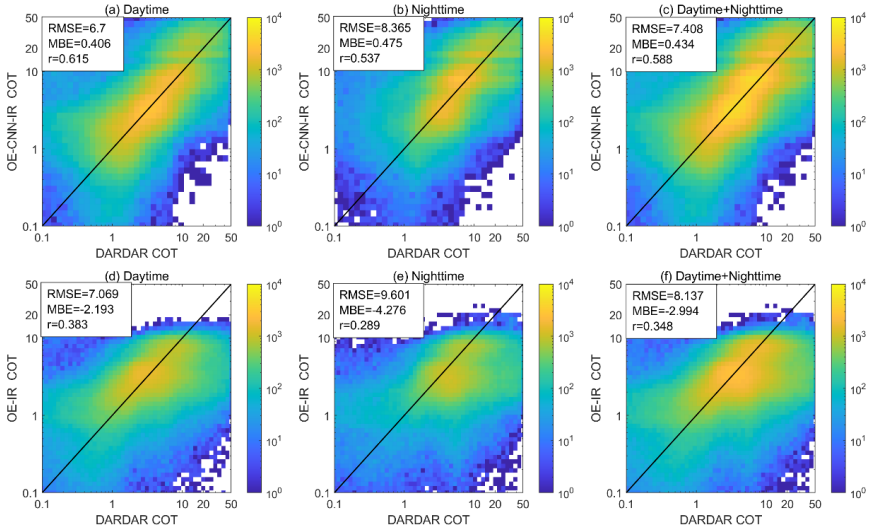

Figure 9. Comparisons of OE-CNN-IR COT, OE-IR COT and DARDAR COT for ice clouds. (a-c) are comparisons between OE-CNN-IR COT and DARDAR products. (d-f) are comparisons between OE-IR COT and DARDAR products. The left column is for daytime comparisons, the middle column is for nighttime comparisons, and the right column is for all-day comparisons.

4 Conclusions

This study introduces a cloud property retrieval method based on optimal estimation (OE-CNN-IR), which integrates traditional radiative transfer simulations with a machine-learning method. Designed for retrieving COT, CER, and CTH, this method is applicable for passive satellite imagery under both daytime and nighttime conditions. Retrievals from a machine learning algorithm (TIR-CNN) are used to provide initial guesses for OE method, and an RTM is used to create radiance lookup tables that are used in the iteration processes. Subsequently, the initial guesses are iteratively adjusted to minimize discrepancies between the IR observations and radiative transfer model simulations. The efficacy of OE-CNN-IR is validated against MYD06 products and active sensor cloud products, and the results are compared to a stand-alone optimal estimation model (OE-IR).

The validation results reveal that the OE-CNN-IR method outperforms stand-alone OE-IR model, especially for cloud optical thickness of thick clouds. Correlation coefficients with MYD06 products have exhibit marked improvements: correlation coefficients for COT increases from 0.66 to 0.784, correlation coefficients for CER increases from 0.364 to 0.517, and correlation coefficients for CTH increases from 0.792 to 0.846. In nighttime evaluations, the OE-CNN-IR method consistently

https://doi.org/10.5194/amt-2024-36
Preprint. Discussion started: 8 March 2024

outperforms the traditional OE model when compared with DARDAR COT. The consistency between OE-CNN-IR retrievals and MYD06 products is not as good as that of stand-alone machine-learning retrieval algorithm (i. e., TIR-CNN), but the radiance simulations based on OE-CNN-IR retrievals exhibit greater consistency with actual observations, as depicted in Fig. 4. Prospects for enhancing the accuracy of this novel retrieval method lie in future advancements of radiative transfer models. Furthermore, the algorithm explicitly addresses physical processes, aligning with the preferences of scientists who advocate for physically based methodologies. While the OE-CNN-IR method in this study is primarily applied to Aqua-MODIS imagery, it can be potentially applied to other sensors with similar infrared (IR) channels. For instance, it can be readily adapted to geostationary satellites, given their analogous wavelength ranges(Tana et al., 2023, Zhao et al. 2023). In the future, the combination of machine-learning algorithms and traditional radiative transfer simulations might be further developed in other fields of remote sensing.

Code/Data availability

The custom code/data used in this study is available upon reasonable request from the corresponding author.

Competing interests

The authors declare that they have no conflict of interest.

CRediT authorship contribution statement

He Huang: Methodology, Data curation, Validation, Formal analysis. **Quan Wang:** Data curation, Writing – review & editing. **Chao Liu:** Writing – review & editing. **Chen Zhou:** Conceptualization, Methodology, Validation, Writing – review & editing, Supervision.

Acknowledgement

This work was supported by the National Natural Science Foundation of China (Grant No. NSFC 42075127 and 42375038), and the AI & AI for Science Project of Nanjing University.

https://doi.org/10.5194/amt-2024-36
Preprint. Discussion started: 8 March 2024

References

Arking, A. and Childs, J. D.: Retrieval of Cloud Cover Parameters from Multispectral Satellite Images, J. Appl. Meteor. Climatol., 24, 322–334, doi:10.1175/1520-0450, 1985.

Bai, H., Zheng, Z., Zhang, Y., Huang, H., and Wang, L.: Comparison of Satellite-based $PM_{2.5}$ Estimation from Aerosol Optical Depth and Top-of-atmosphere Reflectance, Aerosol Air Qual. Res., 21, 1–17, doi:10.4209 /aaqr.2020.05.0257, 2021.

Guo, C., Ai, W., Hu, S., Du, X., & Chen, N.: Sea surface wind direction retrieval based on convolution neural network and wavelet analysis, IEEE Journal of Selected Topics in Applied Earth Observations and Remote Sensing, 15, 3868-3876, doi:10.1109/JSTARS.2022.3173001, 2022.

Häkansson, N., Adok, C., Thoss, A., Scheirer, R., and Hörnquist, S.: Neural network cloud top pressure and height for MODIS, Atmos. Meas. Tech., 11, 3177–3196, doi:10.5194/AMT-11-3177-2018, 2018.

Hamada, A. and Nishi, N.: Development of a cloud-top height estimation method by geostationary satellite split-window measurements trained with cloudsat data, J. Appl. Meteorol. Climatol., 49, 2035–2049, doi:10.1175/2010JAMC2287.1, 2010.

Han Yong, Paul van Delst, Quanhua Liu, Fuzhong Weng, Banghua Yan, Russ Treadon, and J. D.: JCSDA Community Radiative Transfer Model (CRTM) : Version 1, NOAA Technical Report NESDIS, 122, 2006.

Harshvardhan, Zhao, G., Di Girolamo, L., and Green, R. N.: Satellite-observed location of stratocumulus cloud-top heights in the presence of strong inversions, IEEE Transactions on Geoscience and Remote Sensing, 47, 1421–1428, doi:10.1109/TGRS.2008.2005406, 2009.

IWABUCHI, H., PUTRI, N. S., SAITO, M., TOKORO, Y., SEKIGUCHI, M., YANG, P., and BAUM, B. A.: Cloud Property Retrieval from Multiband Infrared Measurements by Himawari-8, Journal of the Meteorological Society of Japan. Ser. II, 96B, 27–42, doi:10.2151/jmsj.2018-001, 2018.

Lai, R., Teng, S., Yi, B., Letu, H., Min, M., Tang, S., and Liu, C.: Comparison of cloud properties from Himawari-8 and FengYun-4A geostationary satellite radiometers with MODIS cloud retrievals, Remote Sens., 11,1703, doi:10.3390/rs11141703, 2019.

Li, D., Saito, M., Yang, P., Loeb, N. G., Smith, W. L., & Minnis, P.: On the Scattering-Angle Dependence of the Spectral Consistency of Ice Cloud Optical Thickness Retrievals Based on Geostationary Satellite Observations, IEEE Transactions on Geoscience and Remote Sensing, 61, 1-12, doi:10.1109/TGRS.2023.3331970, 2023.

https://doi.org/10.5194/amt-2024-36
Preprint. Discussion started: 8 March 2024

Liou, K. N. and Davies, R.: Radiation and Cloud Processes in the Atmosphere, Phys Today, 46, 66–67, doi:10.1063/1.2809044, 1993.

Marchand, R., Mace, G. G., Ackerman, T., and Stephens, G.: Hydrometeor detection using Cloudsat - An earth-orbiting 94-GHz cloud radar, J. Atmos. Oceanic Technol., 25, 519–533, doi:10.1175/2007JTECHA1006.1, 2008.

Menzel, W. P., Frey, R. A., Zhang, H., Wylie, D. P., Moeller, C. C., Holz, R. E., Maddux, B., Baum, B. A., Strabala, K. I., & Gumley, L. E.: MODIS global cloud-top pressure and amount estimation: Algorithm description and results, Journal of Applied Meteorology and Climatology, 47(4), 1175-1198, doi:10.1175/2007JAMC1705.1, 2008

Min, M., Li, J., Wang, F., Liu, Z., and Menzel, W. P.: Retrieval of cloud top properties from advanced geostationary satellite imager measurements based on machine learning algorithms, Remote Sens., Environ., 239, 111616, doi:10.1016/j.rse.2019.111616, 2020.

Minnis, P., Sun-Mack, S., Young, D. F., Heck, P. W., Garber, D. P., Chen, Y., ... & Yang, P.: CERES edition-2 cloud property retrievals using TRMM VIRS and Terra and Aqua MODIS data—Part I: Algorithms, IEEE Transactions on Geoscience and Remote Sensing, 49(11), 4374-4400, doi: 10.1109/TGRS.2011.2144601, 2011.

Nakajima, T., and M. D. King: Determination of the Optical Thickness and Effective Particle Radius of Clouds from Reflected Solar Radiation Measurements. Part I: Theory, J. Atmos. Sci., 47, 1878–1893, doi:10.1175/1520-0469, 1990

Painemal, D. and Zuidema, P.: Assessment of MODIS cloud effective radius and optical thickness retrievals over the Southeast Pacific with VOCALS-REx in situ measurements, Journal of Geophysical Research Atmospheres, 116, 1–16, doi:10.1029/2011JD016155, 2011.

Poulsen, C. A., Siddans, R., Thomas, G. E., Sayer, A. M., Grainger, R. G., Campmany, E., Dean, S. M., Arnold, C., and Watts, P. D.: Cloud retrievals from satellite data using optimal estimation: Evaluation and application to ATSR, Atmos. Meas. Tech., 5, 1889–1910, doi:10.5194/AMT-5-1889-2012, 2012.

Rodgers, C. D.: Inverse methods for atmospheric sounding: theory and practice, Vol.2., World scientific, 2000.

Rossow, W. B., L. C. Garder, and A. A. Lacis.: Global, Seasonal Cloud Variations from Satellite Radiance Measurements. Part I: Sensitivity of Analysis, J. Climate, **2**, 419–458, doi:10.1175/1520-0442, 1989.

https://doi.org/10.5194/amt-2024-36
Preprint. Discussion started: 8 March 2024

Sassen, K., Wang, L., Starr, D. O., Comstock, J. M., and Quante, M.: A midlatitude cirrus cloud climatology from the facility for atmospheric remote sensing. Part V: Cloud structural properties, J. Atmos. Sci., 64, 2483–2501, doi:10.1175/JAS3949.1, 2007.

Sassen, K., Wang, Z., and Liu, D.: Global distribution of cirrus clouds from CloudSat/cloud-aerosol lidar and infrared pathfinder satellite observations (CALIPSO) measurements, Journal of Geophysical Research Atmospheres, 114, 1–12, doi:10.1029/2008JD009972, 2009.

Shi, C., Hashimoto, M., and Nakajima, T.: Remote sensing of aerosol properties from multi-wavelength and multi-pixel information over the ocean, Atmos. Chem. Phys., 19, 2461–2475, doi:10.5194/acp-19-2461-2019, 2019.

Shi, C., Hashimoto, M., Shiomi, K., & Nakajima, T.: Development of an algorithm to retrieve aerosol optical properties over water using an artificial neural network radiative transfer scheme: First result from GOSAT-2/CAI-2, IEEE Transactions on Geoscience and Remote Sensing, 59(12), 9861-9872, doi:10.1109/TGRS.2020.3038892, 2020.

Stubenrauch, C. J., A. Chédin, G. Rädel, N. A. Scott, and S. Serrar: Cloud properties and their seasonal and diurnal variability from TOVS Path-B, J. Climate, 19, 5531–5553, doi:10.1175/JCLI3929.1, 2006.

Tan, Z., Ma, S., Liu, C., Teng, S., Letu, H., Zhang, P., & Ai, W.: Retrieving cloud base height from passive radiometer observations via a systematic effective cloud water content table. Remote Sensing of Environment, 294, 113633, doi:10.1016/j.rse.2023.113633, 2023.

Tan, Z., Ma, S., Liu, C., Teng, S., Xu, N., Hu, X., ... & Yan, W.: Assessing overlapping cloud top heights: An extrapolation method and its performance, IEEE Transactions on Geoscience and Remote Sensing, 60, 1-11, doi:10.1109/TGRS.2022.3170054, 2022.

Tana, G., Ri, X., Shi, C., Ma, R., Letu, H., Xu, J., and Shi, J.: Retrieval of cloud microphysical properties from Himawari-8/AHI infrared channels and its application in surface shortwave downward radiation estimation in the sun glint region, Remote Sens. Environ., 290, doi:10.1016/j.rse.2023.113548, 2023.

Twomey, S., and K. J. Seton: Inferences of gross microphysical properties of clouds from spectral reflectance measurements, J. Atmos. Sci., 37, 1065–1069, doi:10.1175/1520-0469, 1980.

Wang, J. and Christopher, S. A.: Intercomparison between satellite-derived aerosol optical thickness and $PM_{2.5}$ mass: Implications for air quality studies, Geophysical Research Letters, 30, 21, doi:10.1029/2003GL018174, 2003.

https://doi.org/10.5194/amt-2024-36
Preprint. Discussion started: 8 March 2024


Atmospheric Measurement Techniques Discussions

Wang, Q., Zhou, C., Zhuge, X., Liu, C., Weng, F., and Wang, M.: Retrieval of cloud properties from thermal infrared radiometry using convolutional neural network, Remote Sens. Environ., 278, 113079, doi:10.1016/j.rse.2022.113079, 2022.

Wang, Q., Zhou, C., Letu, H., Zhu, Y., Zhuge, X., Liu, C., Weng, F., and Wang, M.: Obtaining Cloud Base Height and Phase from Thermal Infrared Radiometry Using a Deep Learning Algorithm, IEEE Transactions on Geoscience and Remote Sensing, 61, doi:10.1109/TGRS.2023.3317532, 2023.

Yang, P., Tsay, S.-C., Wei, H., Guo, G., and Ji, Q.: Remote sensing of cirrus optical and microphysical properties from ground-based infrared radiometric Measurements-part I: a new retrieval method based on microwindow spectral signature, IEEE Geoscience and Remote Sensing Letters, 2, 128–131, doi:10.1109/LGRS.2005.844733, 2005.

Yuan, Q., Shen, H., Li, T., Li, Z., Li, S., Jiang, Y., Xu, H., Tan, W., Yang, Q., Wang, J., Gao, J., and Zhang, L.: Deep learning in environmental remote sensing: Achievements and challenges, Remote Sensing of Environment, 241, 111716, doi:10.1016/j.rse.2020.111716, 2020.

Zhao, C., Xie, S., Klein, S. A., Protat, A., Shupe, M. D., McFarlane, S. A., Comstock, J. M., Delano, J., Deng, M., Dunn, M., Hogan, R. J., Huang, D., Jensen, M. P., MacE, G. G., McCoy, R., O'Connor, E. J., Turner, D. D., and Wang, Z.: Toward understanding of differences in current cloud retrievals of ARM ground-based measurements, Journal of Geophysical Research: Atmospheres, 117, doi:10.1029/2011JD016792, 2012.

Zhao, H., Li, R., Zhang, P., Fu, Y., Yang, S., Huang, C., & Li, D.: Satellite-Based Fully Connected Neural Network Heating (FCNH) Algorithm for Estimating Latent Heating Rate Inside Storms. Journal of Geophysical Research: Atmospheres, 128(19), doi:10.1029/2022JD038448, 2023.

Zou, X., Zhuge, X., and Weng, F.: Characterization of bias of Advanced Himawari Imager infrared observations from NWP background simulations using CRTM and RTTOV, J. Atmos. Ocean Technol., 33, 2553–2567, doi:10.1175/JTECH-D-16-0105.1, 2016.